

The Possible Protective Role of Selenium Nano-particles Against Gentamicin-Induced Toxicity in The Testis of the Adult Male Albino Rat: Histological and Immunohistochemical Study

Hala Taha Shalan and Yasmin Ramadan Abd El Fattah

Department of Anatomy and Embryology, Ain Shams University, Faculty of Medicine, Egypt

ABSTRACT

Introduction: Gentamicin (GM) is a potent bactericidal, broad-spectrum aminoglycoside. Selenium nanoparticles (SeNPs) are featured with improved antioxidant ability compared to other chemical forms of selenium with reducing the risk of selenium toxicity.

Aim of the Work: The current work attempted to evaluate the possible protective contribution of selenium nanoparticles to gentamicin-induced toxicity in the testis of rat.

Material and Methods: 36 adult male albino rats were included in the current research. Their age ranges between 3-5 months and their weight (180-220g). Rats were categorized into three groups. Group I: It was composed of 12 rats, that were divided into three equivalent subgroups; Subgroup IA: comprising 4 rats maintained a negative control and received nothing but food and water for 6 days; Subgroup IB: included 4 rats that received 0.5 mg/kg intraperitoneal (IP) saline for 6 successive days and Subgroup IC included 4 rats that received selenium nanoparticles 0.5 mg/kg intraperitoneal (IP) for 6 successive days. Group II: It included twelve adult male rats that received gentamycin 100 mg/kg IP for 6 successive days. Group III: It included twelve rats that received both gentamicin and selenium nanoparticles. IP selenium nanoparticles will be administered to rats 1hr after the gentamicin treatment at the same dose and duration mentioned before. The serum testosterone level was determined. Sections of testis underwent histological, biochemical, morphometric and statistical analysis.

Results: Gentamycin induced a significant reduction in testosterone level and degeneration of the spermatogenic epithelial series with large areas of vacuolations, as well as thick and irregular basement membrane. Ki67 count was recorded. Injection of SeNPs enhanced the aforementioned aspects.

Conclusion: GM resulted in histological as well as biochemical changes in the testes of adult male rats. Administration of SeNPs with GM attenuated these negative impacts which can be attributed to the antioxidant activity.

Received: 12 July 2021, **Accepted:** 16 September 2021

Key Words: Gentamycin, nano-selenium, Ki6, testis.

Corresponding Author: Hala Taha Shalan, PhD, Department of Anatomy and Embryology, Ain Shams University, Faculty of Medicine, Egypt, **Tel.:** +20 10 0197 0159, **E-mail:** halashalan1986@yahoo.com

ISSN: 1110-0559, Vol. 46, No.1

INTRODUCTION

It was observed that oligospermia is the one of the most prevalent cause of decreased male fertility. Oligozoospermia is defined as a medical state featured by decreased sperm count as well as reduced quality, which contributes to 90% of male infertility^[1]. Based on the International Committee for Monitoring Assisted Reproductive Technology, World Health, Organization (WHO), infertility is diagnosed as a disease of reproductive system defined by the failure to achieve the clinical pregnancy after 12 months or more of frequent unprotected sexual intercourse^[2].

Gentamicin (GM) is a potent broad-spectrum bactericidal aminoglycoside that acts via the inhibition of protein synthesis. It is frequently used by andrologist and in *vitro* fertilization infection treatment or when elevated leukocyte concentrations are present in patient's semen^[3]. Oxidative stress plays a significant role in the pathogenesis of reproductive disorders, male infertility as well as defective sperm function^[4].

It is assumed that lipid peroxidation as well as oxidative stress could be included in the testicular toxicity of gentamycin in rats and the mixture of drug delivery with strong antioxidant agents could be a convenient method to alleviate the toxic detrimental impacts of gentamycin^[5].

Selenium is known to be an antioxidant. Nanoparticle characteristics, for instance; size, surface charge, as well as hydrophobicity affect their mucosal absorption as smaller particles showed higher cellular uptake^[6]. SeNPs have a wide range in biomedical applications as a nutritional and health improving supplements. SeNPs possess more effective antioxidant ability compared to other chemical forms of selenium regarding alleviating the risks of selenium toxicity. Selenium nanoparticle has been reported as a drug carrier and tumor therapeutic element^[7,8].

Consequently, this research attempted to investigate the possible protective impact of SeNPs on gentamicin toxicity in testes.

MATERIALS AND METHODS

Chemicals

Gentamicin is in the form of ampoules of 2 ml 40 mg/mL of gentamicin sulphate. It is manufactured by Memphis Co. for Pharm. and Chem. Ind. (MEMCO), Egypt; under the authority of Schering Plough Corporation, U.S.A., Cairo, Egypt.

SeNPs (40-45 nm particle size) were purchased from Nano-Tech Egypt for Photo-Electronic, 6 October, Al Giza Egypt, as a sterile solution, dispersed in phosphate-buffered saline (PBS) and ready to be used.

Animals

The current study was performed on 36 adult albino rats, their age ranges between 3-5 months and their weight between (180-220g). The rats were purchased from the Medical Ain Shams Research Institute (MASRI). Rats were housed for one week for environmental adaptation under standard laboratory conditions on a 12-hour light/dark cycle. They received an adequate and constant diet along with free access to water ad libitum. Rats were kept isolated for two weeks in a laboratory room at comfortable room temperature for adaptation before any experiments. Moreover, all experiments were conducted during the same time of the day, between 8 a.m. and 2 p.m. to avoid variations because of diurnal rhythms.

Ethical Consideration

All the experiments were performed based on the guidelines issued by the Animal Research Ethics Committee of Ain Shams University Faculty of Medicine. The procedure was performed based on the Ethical Guidelines for experimental pain diagnosis in conscious animals^[9].

Experimental Protocol

Rats were randomly categorized into three Groups:

Group I (Control Group): 12 rats which were subdivided into three subgroups, four rats each:

- Group I-a (negative control): four rats did not undergo any experiments, receiving only food and water for 6 days.
- Group I-b (positive control): four rats received 0.5 mg/kg intraperitoneal (IP) saline for 6 successive days.
- Group I-c (nanoselenium Group): four rats received SeNPs 0.5 mg/kg intraperitoneal (IP) for 6 successive days^[10].

Group II (GM-treated group): twelve rats received GM 100 mg/kg IP for 6 successive days^[3].

Group III (GM+ SeNPs group): twelve rats received both gentamicin and selenium nanoparticles. SeNPs IP will be administered to rats 1hr after the GM treatment at same dose and duration mentioned above.

Before scarification of rats, blood was collected from the tail veins of animals belonging to each group for assessment of serum testosterone. Median abdominal incision was performed, and organs were dissected. Testes were extracted. All rats were sacrificed by cervical dislocation after light ether anesthesia^[11].

Processing of samples

Preparation of paraffin blocks and staining methods

Right testes were preserved in 10% buffered formalin, processed, and embedded in paraffin blocks, sectioned at 5µm, cut and then stained by Hematoxylin and Eosin^[12] to study general histological features of the gland and other sections were stained with PAS stain^[13].

Immunohistochemical study

Ki 67 immunostaining^[14] polyclonal rabbit anti-rat Iry Ab (MKI67/NB110-897171) mg/ml, nuclear reaction, proliferation marker, dilution 1:100-1:500. +ve control tonsil, -ve control omit application of Iry Ab, apply for 60 minutes.

Electron microscopy processing

The left testes were fixed in 2.5% glutaraldehyde solution in 0.1 M cacodylate buffer (pH 7.4) for 2 hours and subsequently fixed for 1-2 hours in osmium tetroxide dissolved in the same buffer. Thereafter, they were dried by passing through a graded series of ethanol as well as in propylene oxide, and then incorporated into epoxy resin. With regard to the embedded blocks, they were divided into semi-thin sections (0.5 µm) by a diamond knife, stained with 1% toluidine blue, examined and photographed. Then, ultrathin sections (80-90 nm) were stained with uranyl acetate as well as lead citrate in order to be examined by JEOL electron microscope (JEOL, Egypt) at 80 kV in EM Unit, Faculty of Medicine, Al-Azhar University^[15,16].

Morphometric Study

1. Image Analysis

Count of +ve nuclei in Ki 67 were done in immunostained sections work via the computer-aided image analysis system Leica Qwin 500 LTD (Cambridge, UK), count of +ve nuclei in Ki 67 were done in immunostained sections using interactive measurements menu. Data was measured in 10 high power fields. Measurements were made by means of Leica image analyzer (Q 500 MC program, Wetzlar, Germany).

2. Statistical Analysis

The statistical analysis was conducted through the Statistical Package for Social Science (IBM Corp, released 2013. IBM SPSS statistics for windows, V. 22.0. Armonk, NY, USA). Parametric quantitative data were expressed as mean ± standard deviation (SD).

Data were statistically assessed using SPSS/10 software. Methods for hypothesis testing included one-way analysis of variance (ANOVA). ANOVA test was performed to

compare the variance of parametric continuous variable among three categorical independent variables with three or more levels; Bonferroni Post Hoc Tukey test was performed to compare variable with homogeneous variance among two categorical independent variables. All *P values* were two-tailed, the probability (*P-value*) of ≥ 0.05 was statistically non-significant, ≤ 0.05 was statistically significant and ≤ 0.01 was highly statistically significant. All data were expressed as Mean \pm Standard Error of the Mean (SEM).

RESULTS

Histological changes

Group I (control group)

In the present work, no significant differences were detected between the subgroups of group I, therefore the results of three subgroups will be discussed together.

Light microscopy of Hematoxylin and eosin-stained sections of the testes of the control group showed interstitial spaces between the tubules. Different types of spermatogenic cells were seen in order, spermatogonia were detected near the basement membrane, followed by primary spermatocytes and the spermatids appeared smaller than primary spermatocytes and lying close to the lumen. Large spermatozoa occupied the lumen (Figure 1). Semithin stained sections with toluidine blue, revealed the typical histological picture of the seminiferous tubules with normal thickness of the basement membrane and presence of complete spermatogenesis. Spermatogonia were seen close to the basement membrane which was followed by the large primary spermatocytes. Then, the spermatids were smaller than primary spermatocytes and arranged in rows (Figure 2). Higher magnification showed large, rounded spermatocytes. The lumen was occupied by multiple sperms (Figure 3).

PAS-stained sections showed multiple seminiferous tubules with normal thickness to the basement membrane (BM) (Figure 4).

Examination of immunohistochemically stained sections for Ki67 showed few + ve nuclear immune expression (IE) reaction in few interstitial cells (Figure 5).

Electron microscopy of the ultrathin sections of group I testes showed the basal compartment of the seminiferous tubules formed of cells resting on the basement membrane formed of Sertoli cells and spermatogonia. Sertoli cell appeared as a large pyramidal cell having large indented nucleus with prominent nucleolus. Mitochondria were present around the nucleus and appeared away from the basement membrane (Figure 6). Type A dark spermatogonia appeared with oval nuclei containing peripheral clumps of heterochromatin and the tight junctional basal lamina (Figure 7). Primary spermatocytes revealed rounded to oval nuclei containing fine chromatin (Figure 8). The spermatozoa featured their characteristic heads with an electron-dense nucleus and tails (Figure 9).

Group II (gentamycin treated group)

Light microscopy of Hematoxylin as well as Eosin-stained sections of the testes of group II showed signs of degeneration of most spermatogenic cells with areas of depletions. The basement membrane was thick and irregular. There were multiple vacuoles between the germ cells. The interstitial spaces were dilated and showed congested blood vessels (Figure 10). Semithin stained sections with toluidine blue, showed signs of degeneration in spermatogenic cells with pyknotic nuclei and decreased cell density with ill-defined cell boundaries. There were a multiple area of vacuolations in between. The lumen appeared depleted of sperms (Figure 11). Higher magnification showed multiple giant cells and pyknotic cells with large areas of vacuolations (Figure 12).

PAS-stained sections showed an undulating folded BM and thinning BM with focal disruption in some areas (Figure 13).

Examination of immunohistochemically stained sections for Ki67 showed mild + ve nuclear IE reaction in the detected interstitial cells (Figure 14).

Electron microscopy of the ultrathin sections of the testes from the group II revealed some ultrastructural alterations. Primary spermatocyte showed areas of rarified cytoplasmic vacuoles with an irregular basal lamina. There was an increase in electron dense bodies. The sertoli cell was present away from the basement membrane. Mitochondria were the irregularly arranged as they moved away from the basement membrane and mostly occupy the space between basement membrane and the nucleus. (Figure 15). The spermatozoal heads revealed abnormal shapes (Figure 16).

Group III (gentamycin + nanoselenium treated group)

Light microscopy of Hematoxylin as well as Eosin-stained sections of testes in group III showed that although all types of germ cells were observed, few areas of vacuolation and few slightly congested vessels were seen in the interstitial space. The basement membrane of the tubules was slightly appeared normally. In several tubules, there was a restoration of normal spermatogenic lining (Figure 17). Semithin stained sections with toluidine blue, there was significant enhancement in the architecture of the seminiferous tubules with a partial recovery of a germinal epithelium, minimal vacuolations among the germ cells were also detected (Figure 18). Higher magnification showed some large spermatogenic cells with few vacuolations (Figure 19).

PAS stained sections showed that, some tubules appeared with thinning of the BM and others revealed partially thickened BM (Figure 20).

Examination of immunohistochemically stained sections for Ki67 showed +ve sever reaction of nuclear IE was detected in some interstitial (Figure 21).

Electron microscopic examination of the ultrathin sections of the testes from the group III revealed partial preservation of the ultrastructure of spermatogenic cells (Figures 22,23).

Hormonal changes

Serum testosterone was statistically significantly decreased in gentamycin-treated group compared to the control group and the GM+SeNPs treated groups with a

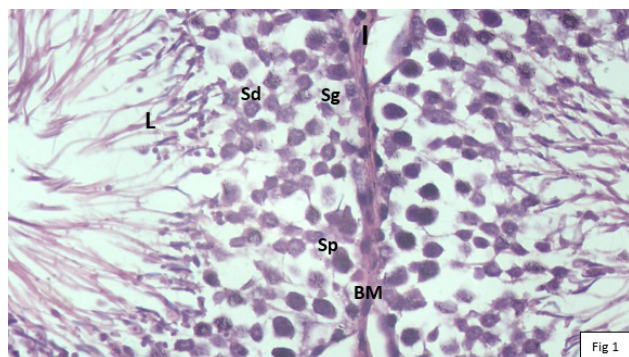


Fig. 1: Photomicrographs of testis of hematoxylin and eosin stained section of group I control group showing seminiferous tubules lined with series of spermatogenic cells; spermatogonia, (Sg) primary spermatocytes (Sp) and round (early) spermatids, (Sd). The lumen (L) of tubules was occupied with sperms. Notice basement membrane (BM) and interstitial space (I). (H@Ex400)

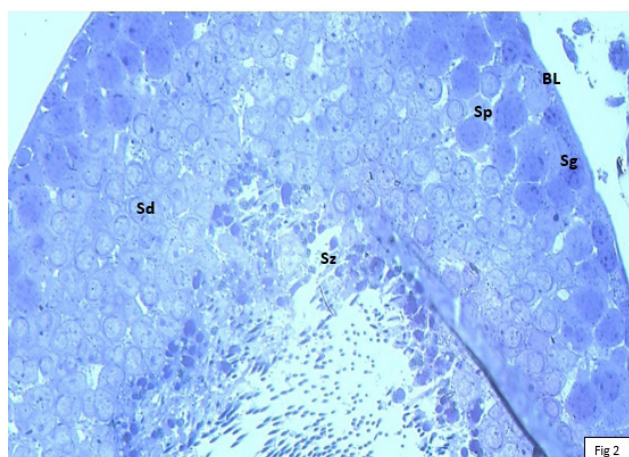


Fig. 2: Photomicrographs of a semithin section of control rat testis showing: spermatogonia (Sg), basal lamina (BL), spermatocytes (Sp), spermatid (Sd), spermatozoa (Sz). (Toluidine blue X400)

P -value <0.001 (Tables 1,2,3 and Histogram 1,2).

Morphometric changes

Regarding the count of Ki67 +vet nuclei, there was a marked elevation in the GM group that was evident compared to the control groups with a P -value <0.001 and a marked elevation in GM+SeNPs group compared to the other groups with a P -value <0.001 (Tables 4,5,6 and Histogram 3,4).

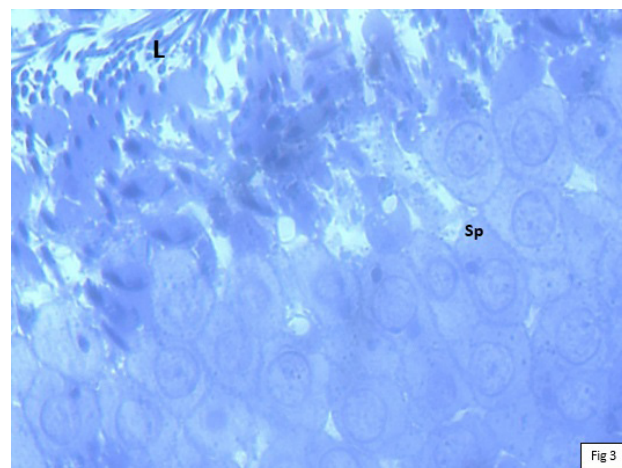


Fig. 3: Higher magnification of photomicrographs of a semithin section of group I control group showing multiple spermatocytes (Sp) with lumen (L) occupied by sperms. (Toluidine blue X1000)

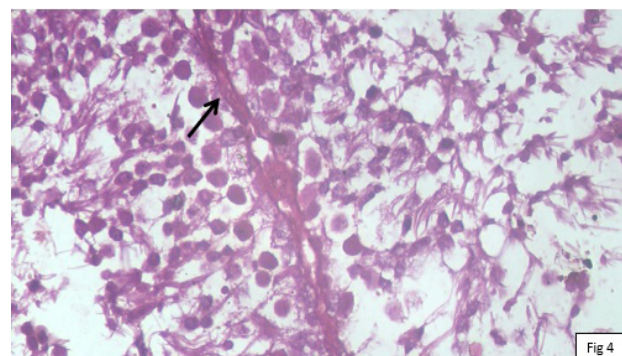


Fig. 4: Sections in the testis of group I rat showing normal thickness of the BM (arrow). (PAS x 400)

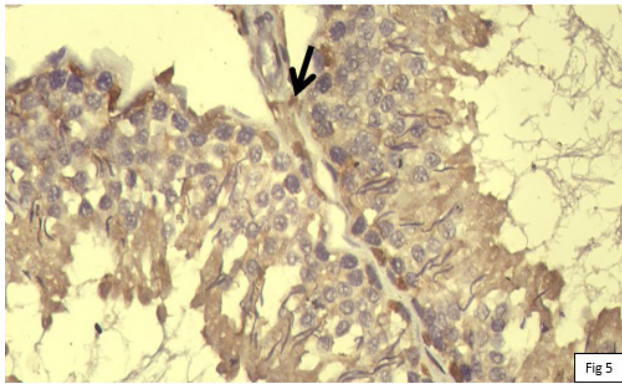


Fig. 5: Sections in the testis of rats group I showing +ve nuclear IE in few interstitial cells (arrow). (Ki67 immunostaining, x 400)

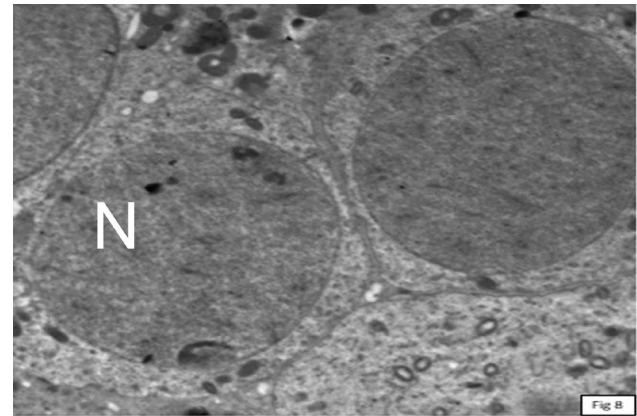


Fig. 8: An electron micrograph of a control rat testis showing a primary spermatocyte with a large rounded to oval nucleus (N) containing fine chromatin. Magnification X2000

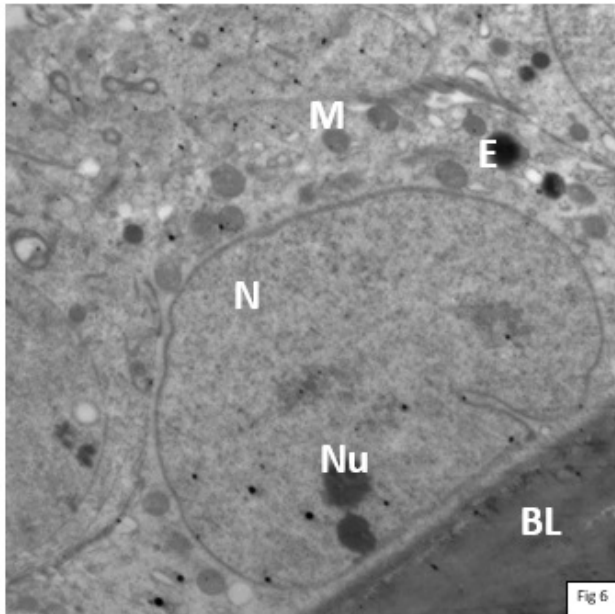


Fig. 6: An electron micrograph of a rat testis of control group showing an apparently normal Sertoli cell present close to the basement membrane having a large indented nucleus (N) with two prominent nucleoli (Nu), mitochondria (M) which present around the nucleus and away from the basement membrane and electron dense body (E). Basal lamina (BL). Magnification X2000

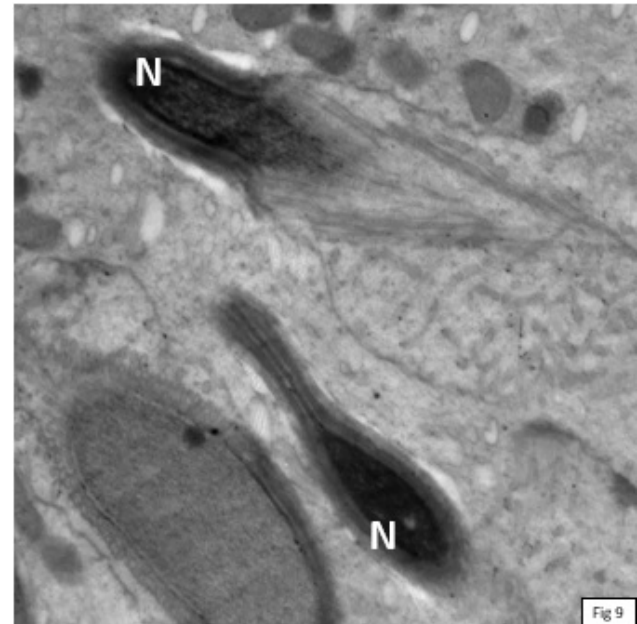


Fig. 9: An electron micrograph of a rat testis of control group showing a normal spermatozoal head with an electron-dense nucleus (N). Magnification, ×4000

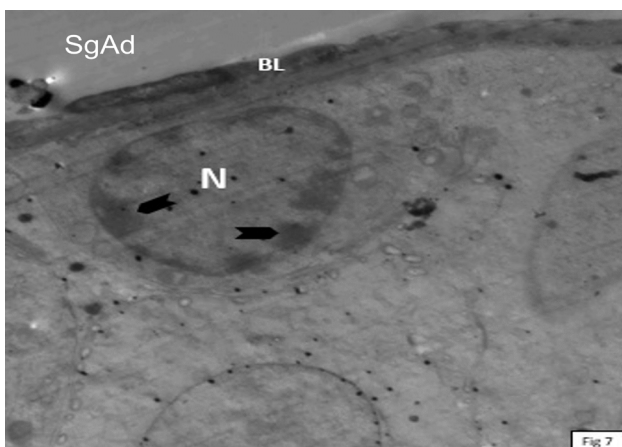


Fig. 7: An electron micrograph of a control rat testis showing type A dark spermatogonium (SgAd) having an oval nucleus (N) with peripheral clumps of heterochromatin (arrowheads). Notice the tight junction basal lamina (BL). Magnification X2000

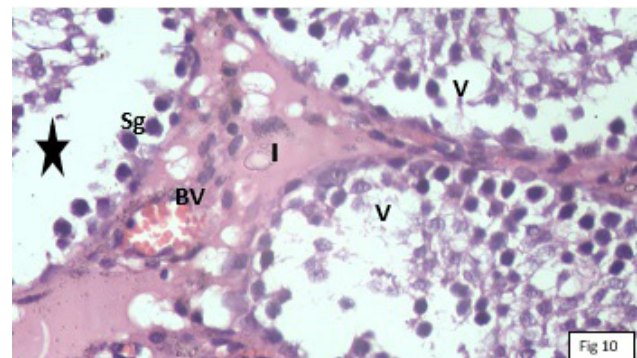


Fig. 10: Photomicrographs of testis of hematoxylin and eosin stained section of group II showing depleted germ cells (star) with areas of vacuolations (V). Notice the wide interstitial space (I) with congested blood vessels (BV). Spermatogenic cells still detected (Sg). H@Ex400

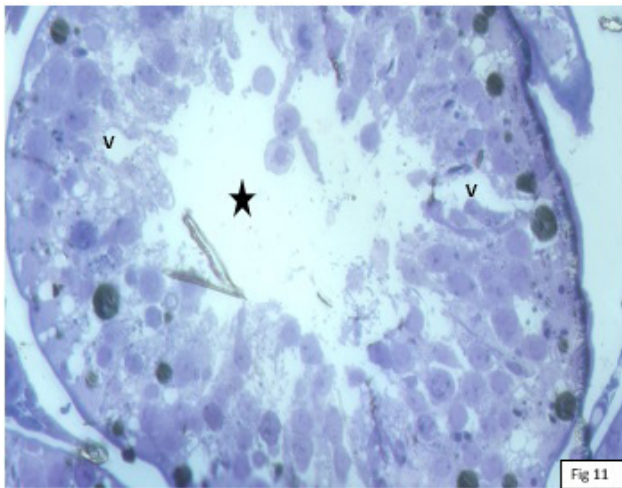


Fig. 11: Photomicrographs of a semithin section of group II showing disorganization of seminiferous tubules with extensive vacuolization (V) of the germinal epithelium. Notice the empty lumen (☆). (Toluidine blue X400)

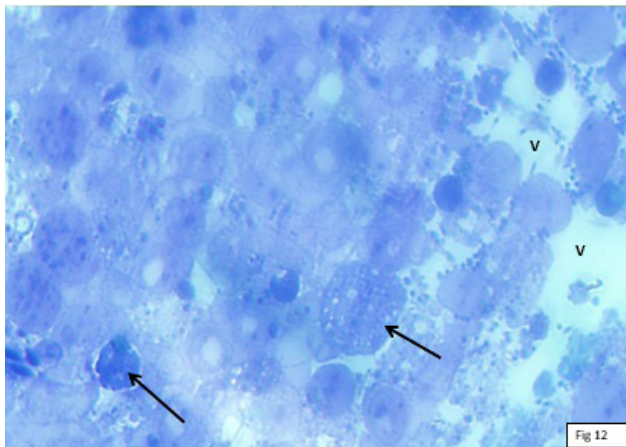


Fig. 12: Higher magnification of photomicrographs of a semithin section of group II showing distortion of the shape of spermatogenic cells, multiple giant cells and pyknotic cells (arrow) with large areas of vacuolations (V). (Toluidine blue X1000)

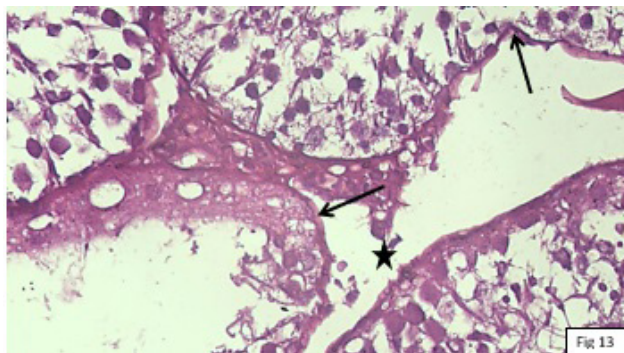


Fig. 13: Sections in the testis of rats group II showing folded BM (arrows) in some tubules and focal disruption (☆) of BM of other tubule. Notice widening in the interstitial space (I). (PAS x 400)

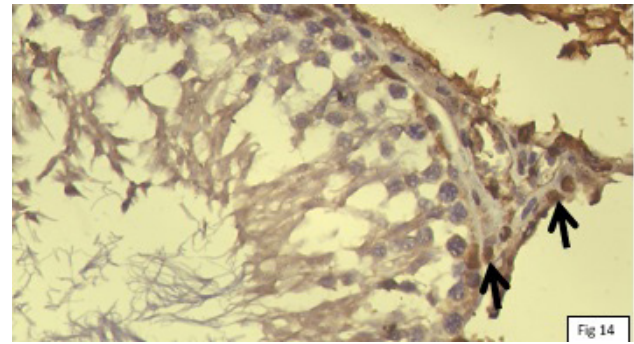


Fig. 14: Sections in the testis of rats group II showing +ve nuclear IE in some interstitial cells (arrow). (Ki67 immunostaining, x 400)

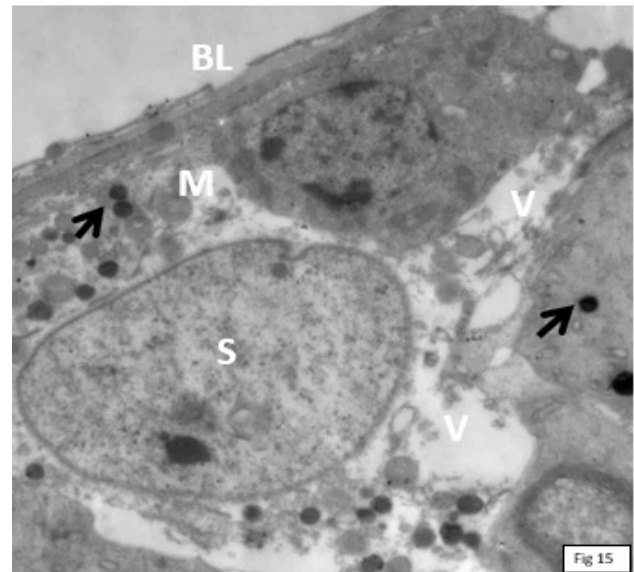


Fig. 15: An electron micrograph of a rat testis of group II showing a primary spermatocyte with areas of rarified cytoplasmic vacuoles (V). Notice the irregular basal lamina (BL). There is an increase in electron dense bodies (arrow). Notice the irregularly arranged mitochondria (M) as most of them occupy the space between basement membrane and the nucleus. The Sertoli cell present away from the basement membrane (S). Magnification, ×2000

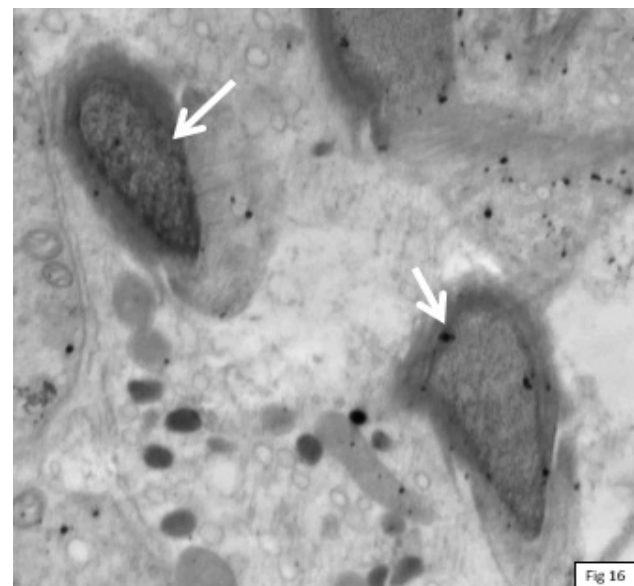


Fig. 16: An electron micrograph of a rat testis of group II showing the spermatozoal heads with abnormal shapes (arrows). Magnification X4000

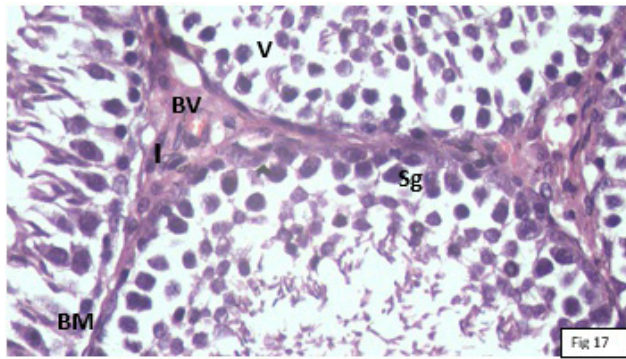


Fig. 17: Photomicrographs of testis of hematoxylin and eosin stained section of group III showing the interstitial space (I) slightly dilated with congested blood vessels (BV). An area of vacuolations was observed (V). Notice the presence of spermatogenic cells (Sg). Basement membrane (BM). (H&E x400)

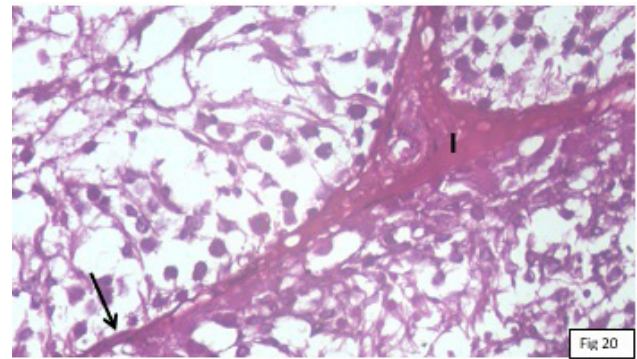


Fig. 20: Sections in the testis of rats group III showing some tubules with normal BM (arrow) and other tubules with partially thickened interstitial space (I) (PAS x 400)

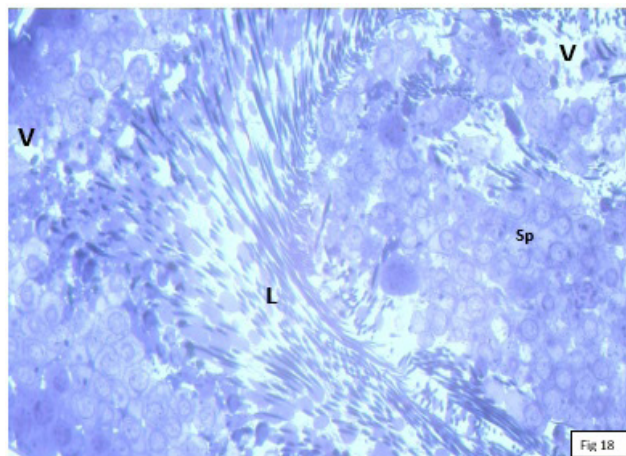


Fig. 18: Photomicrographs of a semithin section of group II showing multiple spermatocytes (Sp). The lumen (L) was occupied by sperms. Areas of vacuolations (V) still detected. (Toluidine blue X400)

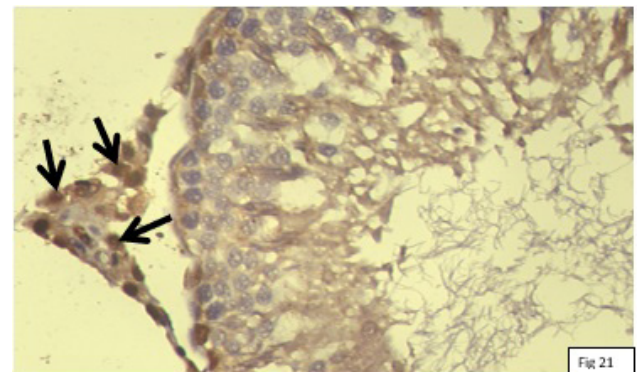


Fig. 21: Sections in the testis of rats group III showing showing +ve nuclear IE in multiple interstitial cells (arrows). (Ki67 immunostaining, x 400)

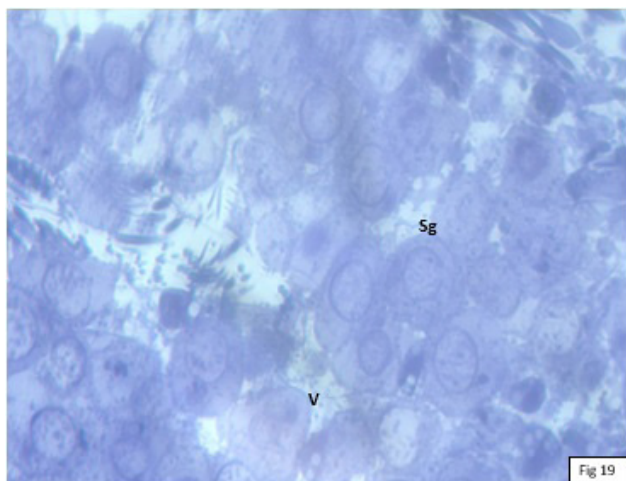


Fig. 19: Higher magnification of photomicrographs of a semithin section of group III showing few areas of vacuolations (V) with restoration to the apparently normal spermatogenic cells (Sg). (Toluidine blue X1000)

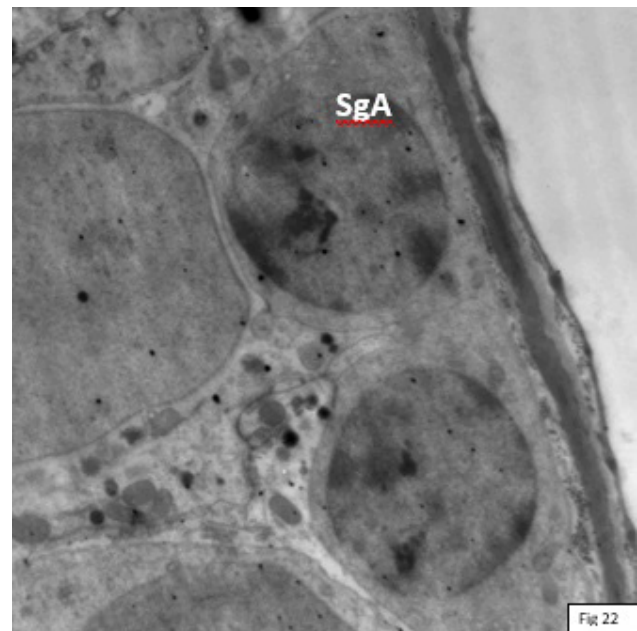


Fig. 22: An electron micrograph of a rat testis of group III showing apparently normal type A spermatogonia (SgA) with rounded nucleus. Magnification x2000

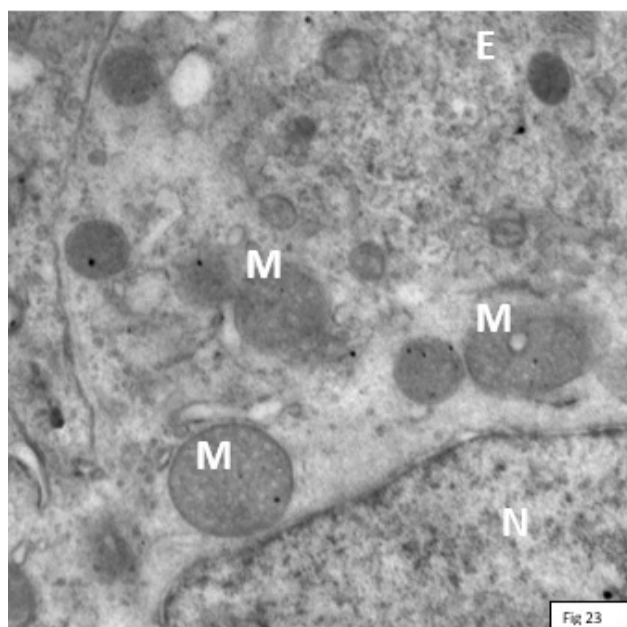


Fig. 23: An electron micrograph of a rat testis of group III showing an apparently normal nucleus of Sertoli cell (N) and mitochondria (M). Notice few electron dense body (E). Magnification, $\times 6000$

Table 1: Descriptive data of Testosterone hormone level (ng/ml)

	N	Mean	SD	Minimum	Maximum
Control	12	1.154	0.279	0.832	1.52
GM	12	0.057	0.035	0.020	0.1
GM + Nano	12	0.900	0.262	0.500	1.2
Total	36	0.703	0.522	0.020	1.52

Table 2: ANOVA test of Testosterone hormone level (ng/ml)

	Control	GM	GM + Nano	P value	Sig
Mean (SD)	1.154 (0.279)	0.057 (0.035)	0.900 (0.262)	<0.001	S

Table 3: Post Hoc Tukey HSD test of Testosterone hormone level (ng/ml)

Group	Group	P value	Sig
Control	GM	<0.001	S
Control	GM + Nano	<0.022	S
GM	GM + Nano	<0.001	S

Table 4: Descriptive data of Ki 67 +nuclei

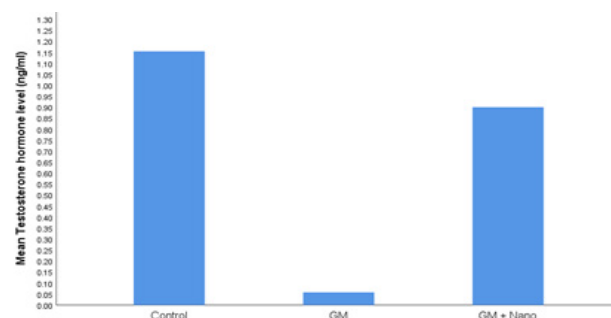
	N	Mean	SD	Minimum	Maximum
Control	12	3.17	1.115	2	5
GM	12	12.33	1.670	10	15
GM + Nano	12	19.50	1	18	21
Total	36	11.67	6.895	2	21

Table 5: ANOVA test of Ki 67 +nuclei

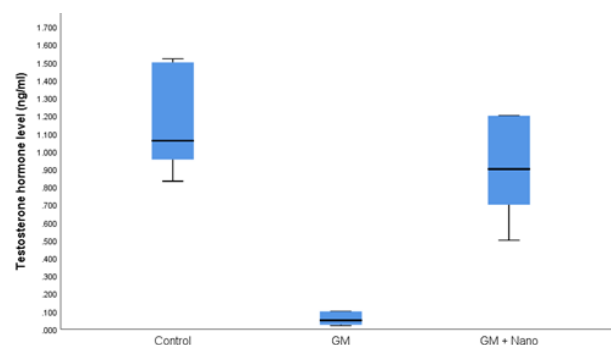
	Control	GM	GM + Nano	P value	Sig
Mean (SD)	3.17 (1.115)	12.33 (1.67)	19.50 (1)	<0.001	S

Table 6: Post Hoc Tukey HSD test of Ki 67 +nuclei

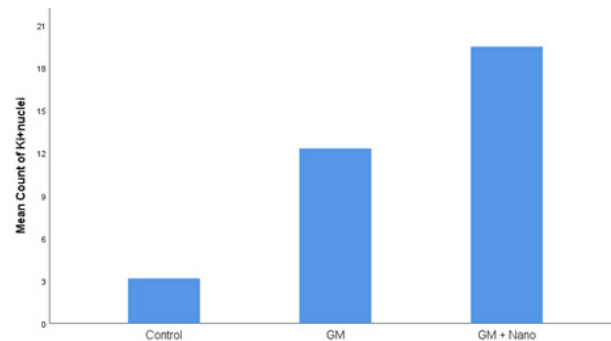
Group	Group	P value	Sig
Control	GM	<0.001	S
Control	GM + Nano	<0.001	S
GM	GM + Nano	<0.001	S



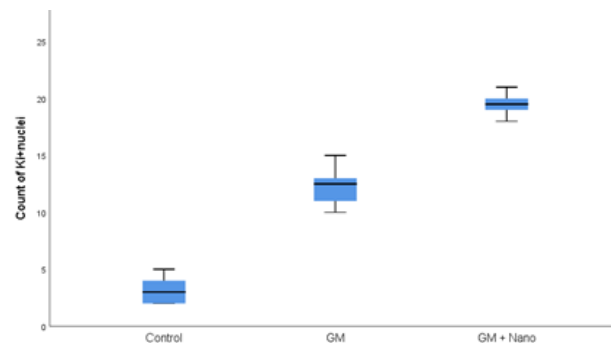
Histogram 1: Bar chart shows the mean of Testosterone hormone level (ng/ml) among three groups



Histogram 2: Boxplot graph for Testosterone hormone level (ng/ml) of the three groups



Histogram 3: Bar chart shows the mean of Ki 67 +nuclei among three groups



Histogram 4: Boxplot graph for Ki 67 +nuclei of the three groups

DISCUSSION

Testis is regarded of the major organs of the reproductive system of males. It is considered highly sensitive to hormonal, genetic as well as environmental substances. Gentamycin is mainly used by urologist but affects male fertility^[17].

In the present study, the immunohistochemical, histological as well as the ultrastructural results of rats of group Ic administrated nanoselenium were similar to the control group Ia and Ib which received no drugs and saline, respectively. This was also reported by Mohammed^[18] who mentioned that the thickness of the germinal epithelium displayed non-significant changes between the control group and the nano selenium treated group.

In the present work, serum testosterone was decreased in GM-treated group than the control group and the GM+SeNPs treated groups. This is compatible with the findings of Mohamed *et al*^[19] who detected that serum testosterone reduction might be due to a disturbed oxidant antioxidant state.

A dose of GM 100 mg / kg IP for 6 successive days in this study also used by Kim *et al*^[3] and Aly and Hassen^[20] who noticed that as the dose and duration of gentamicin administration increased as the testosterone level decreased.

Histological examination of the GM group revealed different morphological alterations in seminiferous tubules, which are characterized by degeneration, reduced cell lining, decreased spermatogenic cells numbers and BM thickening that might act as a direct effect of GM. Mohamed *et al*^[19] demonstrated that testicular testosterone concentration reduction might be the key factor in these degenerative changes. Khaki^[21] mentioned another illustration of gentamicin-induced testicular degeneration which was postulated through ROS generation as the superoxide, H₂O₂ which is commonly utilized in order to induce oxidative as well as necrotic damages.

In the present study, there were vacuoles and cellular debris with almost no spermatogenic cells and their location is left on Sertoli cells. Paniagua *et al*^[22] hypothesized that Sertoli cell vacuolation can be attributed to the abnormal germ cell degeneration. These vacuoles are compatible with the expansion of extracellular vacuoles caused by the premature exfoliation of germ cells.

Cell degeneration of Sertoli cells leads to lipid droplet accumulation in Sertoli cell cytoplasm. These ultra-structural alternations have been detected in progressive testicular reflux with age in males, that might be associated with the hormonal changes present in aging^[22].

With regard to the vacuolated cytoplasm of spermatogenic cells, this could be attributed to lipid peroxidation with consequent damage to the cell membrane caused by GA, as well as cell organelle membranes with a consequent increase in their permeability^[23]. Kumar

et al^[24] reported that the clear vacuoles within the cytoplasm considered distended and pinched-off segments of the endoplasmic reticulum. They also demonstrated that the cellular swelling may occur due to the failure of energy-dependent ion pumps in the plasma membrane, resulting in the inability to maintain ionic and fluid homeostasis, and the study referred this pattern of nonlethal injury is vacuolar dissolution or hydrolysis.

Dilation of interstitial spaces was observed in this study. It was described by El-Sherif and El-Mehi^[25] as they stated that the widening of the intertubular spaces could be attributed to the deposition of the homogeneous acidophilic material in most of the interstitial spaces, which is a hyaline material.

This hyaline material might be due to overabundant lymphatic secretions that exudate from degenerated lymphatic vessels, as well as an increased vascular permeability induced by free radical accumulation along with reactive oxygen species (ROS)^[26].

The widening of the intercellular spaces can also be explained by the disruption of the tight junctions of blood–testis barrier, upon exposure to the ROS, resulting in the ingress of excess water in addition to toxic agents between the spermatogenic cells, with consequent widening of the intercellular spaces^[27]. The loss of cell cohesiveness may be attributed to the damage of the cellular processes of Sertoli cells that fill the gap between the germ cells leading to spermatogenic cell exfoliation into seminiferous tubule lumen^[28].

Shrunken spermatogonia and spermatogonial cell separation from each other and from the basal lamina were also detected in the present work. It can be regarded as pre-apoptotic signs. These results are consistent with those of the testicular epithelium of cisplatin-treated rats. Apoptosis significantly contributes to damaged spermatogonial cell removal in order to prevent abnormal sperm formation. It has been also demonstrated that spermatogenic cells that cannot accomplish the mitotic division are removed by apoptosis^[29].

In the present study, testosterone level was significantly decreased with gentamycin administration. Prior studies have reported apoptosis induction in male germ cell via withdrawal of testosterone and after vasectomy^[30]. Therefore, the reduced thickness of germinal epithelium in the current study can be attributed to the elevated apoptosis due to lower testosterone.

Multivesicular giant cells were detected in the testes of the gentamicin-treated group, giant cells which seem to be a biomarker of testicular atrophy^[31]. This is caused by the spermicidal fusion because of the occurred changes in the intercellular bridges, cytokinesis failure as well as the increased phagocytic capacity of apoptotic spermatogenic cells^[32].

This research detected an asymmetric, undulating and thickened basement membrane of seminiferous tubules

in addition to a wavy and irregular cell membrane in rat treated with gentamicin. The same results have been reported in irradiated rats as well as in efferent ligation^[33].

Changes in basement membrane thickness synthesized by Sertoli as well as myoid cells can be attributed to the myoid cell contraction or the decline in tubular diameter. Alternations in the level of testosterone or epithelium stimulate secretion damage of some factors like prostaglandins or oxytocin inducing the contraction of myoid cells. Additionally, the increased thickness of basement membrane also occurs with age^[34].

The present results revealed the presence of pyknotic nuclei in some spermatogonia. Kroemer *et al*^[35] attributed nuclear pyknosis as a characteristic of apoptosis. In contrast, Kumar *et al*^[24] illustrated that pyknosis is a pattern of nuclear alternations associated with cell necrosis as well as it is featured with nuclear shrinkage along with elevated basophilia as its DNA condenses into a solid, shrunken mass.

Some spermatozoal heads appeared in abnormal shapes. These abnormalities can be due to the disruption of spermatogenesis with consequent deterioration in motility and content of spermatozoa, as well as morphological abnormalities^[36]. Moreover, spermatozoa have been shown to be more vulnerable to oxidative damage as spermatozoa cell membranes have high proportions of polyunsaturated fatty acids, besides their cytoplasm includes reduced scavenging enzyme concentrations^[37].

The present work demonstrated that Nano selenium administration minimized the structural changes of seminiferous tubules induced by gentamicin as evidenced by the histological findings.

In addition, it has been stated that the testes contain many antioxidant enzymes in addition to free radical scavengers to emphasize that the steroidogenic as well as spermatogenic functions of this organ are not influenced. Use of vitamin E supplement and selenium considerably improved sperm motility and viability. Therefore, animals fed a selenium deficient diet show a marked decline in testicular activity and a concomitant loss of germ cells from the germinal epithelium of the testes^[38].

Ki67 is an antigen that is found during different cell cycle. GM effect on testicular cells proliferation was done and assessed by means of Ki67 immunohistochemistry and highest count was measured in the SeNPs group indicating cellular proliferation and repair. It was postulated that the positive expression level of Ki-67 is a good response to spermatogenesis dysfunction^[38].

CONFLICT OF INTERESTS

There are no conflicts of interest

REFERENCES

1. Kumar N, Singh AK: Trends of male factor infertility, an important cause of infertility: A review of literature. *J. Hum. Reprod. Sci.*; 2015 8:191–196.)
2. Ramachandran P, Thamiloviam R, Anbu N, Sivaraman D: Pharmacological investigation of spermatogenic potential of siddha formulation manokara chooranam against gentamicin induced testicular toxicity in wistar rats. *Int J Trans Res Ind Med*, Sep – Dec; 2019,1(3): (P) 07- 127)
3. Kim SH, Lee IC, Baek HS, Shin IS, Moon C, Kim SH, Yun WK, Nam KH, Kim HC, Kim JC: Melatonin prevents gentamicin-induced testicular toxicity and oxidative stress in rats. *Andrologia*; 2014, 46 (9):1032-1040.
4. Kim SH, Lee IC, Lim JH, Moon C, Bae CS, Kim SH, Shin DH, Kim HC, Kim JC: Spermatotoxic effects of a-chlorohydrin in rats. *Lab Anim Res*, 2012, 28:11–16.
5. Kim SH, Lee IC, Baek HS, Shin IS, Moon C, Kim SH, Yun WK, Nam KH, Kim HC & Kim JC: Melatonin prevents gentamicin-induced testicular toxicity and oxidative stress in rats Accepted: September 18, 2013 doi: 10.1111/and.12191 first international journal of andrology
6. Boostani A, Sadeghi AA, Mousavi SN, Ch amaniand M and Kashan N: The Effects of Organic, Inorganic, and Nano-Selenium on Blood Attributes inBroiler Chickens Exposed to Oxidative Stress. *ActaScientiae Veterinariae*; 2015, 43(1264): 1-6.
7. Vekariya KK, Kaur J, Tikoo K: ERa signaling imparts chemotherapeutic selectivity to selenium nanoparticles in breast cancer. *Nanomed Nanotech Biol Med*; 2011, 8(7):1125–1132.
8. Hosnedlova B, Kepinska M, Skalickova S, Fernandez C, Ruttkay-Nedecky B, Peng Q, Baron M, Melcova M, Opatrilova R, Zidkova J, Bjørklund G, Sochor J, Kizek R: Nano-selenium and its nanomedicine applications: a critical review. *Int J Nanomedicine*; 2018, 13:2107-2128.
9. Zimmermann M: Ethical guidelines for investigations of experimental pain in conscious animals. *Pain*, 1983,16, 109-110.
10. Asri-Rezaei S, Nourian A, Shalizar-Jalali A, Najafi G, Nazarizadeh A, Koohestani M, Karimi A: Selenium supplementation in the form of selenium nanoparticles and selenite sodium improves mature male mice reproductive performances. *Iran J Basic Med Sci*; 2018, 21(6):577-585.
11. Iranpour FG, Kheiri S: Coadministration of calcium chloride with lead acetate can improve motility of cauda epididymal spermatozoa in Swiss white mice. *Int J Reprod BioMed*; 2016, 14(2): 141-144.
12. Kiernan JK: Histological and Histochemical methods. In: *Theory and practice*. 3rd ed, Arnold Publisher, London, New York and New Delhy; 2001, 111-162.

13. Bancroft JD, Gamble M: Carbohydrates: In: Theory and practice of histological techniques, 6th. Elsevier Health Sciences, Churchill Livingstone, Edinburgh, London, Oxford, New York, Philadelphia, St Louis, Sydney and Toronto; 2008, 161-186.
14. Ayoob R, Tayyeb G, Azra A, Mohsen M, Shohreh R, Mohammad R: The expression of bax protein in the early stages of spinal cord injury in the sperm cells of rats. Polish Annals of Medicine; 2018, 25(2):196-202
15. Bancroft JD, Stevens A: Theory and practice of histological techniques. 4th ed. Churchill Livingstone: Edinburgh. 1996 P. 433-472.
16. Kuo J: Electron microscopy: methods and protocols. 2nd ed. Totowa, NJ: Humana Press Inc.; 2007.
17. Semet M, Paci M, Saïas-Magnan J, Metzler-Guillemain C, Boissier R, Lejeune H, *et al*: The impact of drugs on male fertility: a review. Andrology; 2017, 5(4):640-63.
18. Mohammed AE: Possible Role of Selenium Nanoparticles on Gentamicin-Induced Toxicity in Rat Testis: Morphological and Morphometric study. EJH DOI: 2019, 10.21608/ejh.9926.1093
19. Mohamed SM, ElHawary NM, Mohamed SF, Hashim NI, Saleh SY, Bakeer MR and Sawiress FA: Effect of stem cell therapy on gentamicin induced testicular dysfunction in rats. J Health Med Informat; 2017, 8:263.
20. Aly HA, Hassan MH: Potential testicular toxicity of gentamicin in adult rats. Biochem Biophysical Research Communications; 2018, 497(1):362-7.
21. Khaki A: Assessment on the adverse effects of Aminoglycosides and Flouroquinolone on sperm parameters and male reproductive tissue: A systematic review. Iran J Reprod Med; 2015, 13(3):125-134.
22. Paniagua R, Nistal M, Sáez FJ, Fraile B: Ultrastructure of the aging human testis. J Electron Microscop Tech. 1991; 19:241-260.
23. Sakr SA, Okdah YA, El-Abd SF: Gibberellin A3-induced histological and histochemical alterations in the liver of albino rats. Sci Asia 2003; 29:327-331.
24. Kumar V, Abbas AK, Aster JC: Robbins basic pathology. 9th ed. Philadelphia, PA: Saunders, Elsevier; 2013.
25. El-Sherif NM, El-Mehi A: Effect of semicarbazide on the testis of juvenile male albino rat. J Interdiscipl Histopathol 2015; 3:9-18.
26. Ravikumar S, Srikumar K: Metabolic dysregulation and inhibition of spermatogenesis by gibberellic acid in rat testicular cells. J Environ Biol 2005; 26:567-569.
27. Mohamed D, Saber A, Omar A, Soliman A: Effect of cadmium on the testes of adult albino rats and the ameliorating effect of zinc and vitamin E. Br J Sci 2014; 11:72-95.
28. Sugandhy O, Pannerdoss S, Suryavathi V: Toxic influence of mercuric chloride on antioxidant system in the testis and epididymis of albino rats. The 10th International Conference on Mercury as a Global Pollutant Halifax, Canada 2011; 29: pp. 45-100.
29. Nejad MD, Abedelahi A, Soleimani-Rad J, Mohammadi -Roshandeh A, Rashtbar M, Azami A: Degenerative effect of cisplatin on testicular germinal epithelium. Adv Pharmaceut Bull.; 2012, 2:173-177.
30. Al-Maghrebi M, Kehinde EO, Anim JT: Survivin down re-gulation is associated with vasectomy-induced spermatogenic damage and apoptosis. Med Princ Pract.; 2011, 449-454.
31. Khattab FK: Histological and ultrastructural studies on the testis of rat after treatment with aluminum chloride. Aust J Basic Appl Sci.; 2007, 1:63-72.
32. Gouda ZA, Selim AO: A possible correlation between the testicular structure and short photoperiod exposure in young albino rats: light and electron microscopic study. Egypt J Histol. 2013; 36:28-38.
33. Sawada H, Esaki M: Electron microscopic observation of 137Cs-irradiated rat testis: production of basal laminae for germ cells, despite their absence. J Electron Microscop (Tokyo). 2003; 52:391-407.
34. Siu MK, Cheng CY: Extracellular matrix: Recent advances on its role in junction dynamics in the seminiferous epithelium during spermatogenesis. Biol Reprod. 2004; 71:375-391.
35. Kroemer G, Galluzzi L, Vandenabeele P, Abrams J, Alnemri ES, Baehrecke EH, *et al*: Classification of cell death: recommendations of the Nomenclature Committee on Cell Death. Cell Death Differ 2009; 16:3-11.
36. Garcia-Leston J, Mendez J, Pasaro E, Laffon B: Genotoxic effects of lead: an updated review. Environ Int 2010; 36:623-636.
37. Hosseinchi M, Soltanlinejad F, Najafi G, Roshangar L: Effect of gibberellic acid on the quality of sperm and in *in vitro* fertilization outcome in adult male rats. Vet Res Forum 2013; 4:259-264.
38. Zhao WP, Wang HW, Liu J, Tan PP, Luo XL, Zhu SQ, Chen XL, Zhou BH: Positive PCNA and Ki67 Expression in the testis correlates with spermatogenesis dysfunction in fluoride-treated rats. Biol Trace Elem Res.; 2018, 186 (2):489-497. Epub head of print.

الملخص العربي

الدور الوقائي المحتمل لجزيئات السيلينيوم النانوية ضد السمية التي يسببها الجنتاميسين في خصية الجرذ الذكر البالغ: (دراسة هستولوجية وهستوكيميائية مناعية)

هالة طه شعلان، ياسمين رمضان عبد الفتاح

قسم التشريخ وعلم الأجنة ، كلية الطب ، جامعة عين شمس ، مصر

مقدمة: الجنتاميسين (GM) مبيد قوي للجراثيم، واسع الطيف. تتميز جزيئات السيلينيوم النانوية (SeNPs) بقدرتها على مقاومة الأكسدة المحسنة مقارنة بالأشكال الكيميائية الأخرى للسيلينيوم مع تقليل مخاطر سمية السيلينيوم. الهدف: يهدف العمل الى تقييم المساهمة الوقائية المحتملة لجسيمات السيلينيوم النانوية في السمية التي يسببها الجنتاميسين في خصية الفئران.

المواد والطرق: تم استخدام ٣٦ من ذكور الجرذان البيضاء في البحث وتتراوح أعمارهم بين ٣-٥ أشهر ووزنهم (١٨٠-٢٢٠ جم). تم تصنيف الفئران إلى ثلاث مجموعات. المجموعة الأولى: تتكون من ١٢ جرذاً، تم تقسيمها إلى ثلاث مجموعات فرعية متكافئة. المجموعة الفرعية IA: حافظت ٤ فئران على تحكم سلبي ولم تتلق سوى الطعام والماء لمدة ٦ أيام؛ المجموعة الفرعية IB: تضمنت ٤ جرذان تلقت ٠,٥ مجم / كجم من محلول ملحي (IP) لمدة ٦ أيام متتالية، وتضمنت المجموعة الفرعية IC ٤ فئران تلقت جزيئات السيلينيوم النانوية ٠,٥ مجم / كجم (IP) لمدة ٦ أيام متتالية. المجموعة الثانية: اشتملت على اثني عشر ذكوراً من الجرذان البالغة التي تلقت جنتاميسين ١٠٠ ملجم / كجم IP لمدة ٦ أيام متتالية. المجموعة الثالثة: اشتملت على اثني عشر فأراً تلقت كلا من الجنتاميسين والسيلينيوم النانوية. سيتم إعطاء جزيئات السيلينيوم النانوية IP للجرذان بعد ساعة واحدة من علاج الجنتاميسين بنفس الجرعة والمدة المذكورة من قبل. تم تحديد مستوى هرمون التستوستيرون في الدم. خضعت أقسام الخصية للتحليل النسيجي والكيميائي الحيوي والمورفومتري والإحصائي.

النتائج: أظهرت النتائج تسبب الجنتاميسين في انخفاض كبير في مستوى هرمون التستوستيرون وتنكس في السلسلة الظهارية المولدة للحيوانات المنوية مع وجود مساحات كبيرة من الفجوات، وكذلك غشاء قاعدي سميك وغير منتظم. عزز حقن SeNPs الجوانب المذكورة أعلاه.

الخلاصة: أدى استخدام الجنتاميسين إلى تغيرات نسيجية وكيميائية حيوية في خصيتين ذكور الجرذان البالغة. أدى استخدام الجنتاميسين والسيلينيوم النانوية إلى تخفيف هذه التأثيرات السلبية التي يمكن أن تُعزى إلى نشاط مضادات الأكسدة.